Article

A high efficient electrochemiluminescence resonance energy transfer system in one nanostructure: its application for ultrasensitive detection of microRNA in cancer cells

Zhaoyang Li, Zongfan Lin, Xiaoyu Wu, Haotian Chen, Yaqin Chai, and Ruo Yuan

Anal. Chem., **Just Accepted Manuscript** • Publication Date (Web): 10 May 2017

A high efficient electrochemiluminescence resonance energy transfer system in one nanostructure: its application for ultrasensitive detection of microRNA in cancer cells

Zhaoyang Li, Zongfan Lin, Xiaoyu Wu, Haotian Chen, Yaqin Chai*, Ruo Yuan*

Key Laboratory of Luminescent and Real-Time Analytical Chemistry, Ministry of Education, School of Chemistry and Chemical Engineering, Southwest University, Chongqing 400715, P.R. China

* Corresponding author. Tel.: +86-23-68252277; Fax: +86-23-68253172.

E-mail address: yqchai@swu.edu.cn; yuanruo@swu.edu.cn

ABSTRACT: The electrochemiluminesce (ECL) efficiency of luminous emitter can be enhanced by the means of electrochemiluminesce resonance energy transfer (ECL-RET) with a matched donor. However, generally, the donor and acceptor pairs were separated in different independent nanostructures, experiencing the challenging issues of limited energy transfer efficiency and luminous stability. Herein, we designed novel ECL-RET model within one nanostructure containing the donor of Tris (4,4'-dicarboxylicacid-2,2'-bipyridyl) ruthenium(II) dichloride ($Ru(dcbpy)_3^{2+}$) and the acceptor of CdSe@ZnS quantum dots (QDs) for acting as the ECL emitter ($QDs\text{-}Ru(dcbpy)_3^{2+}$), which significantly reduced the energy loss and improved the ECL efficiency of QDs because of the short path of energy transmission. To demonstrate the proof-of-concept, the proposed $QDs\text{-}Ru(dcbpy)_3^{2+}$ was employed to construct a new kind of ECL biosensor that could achieve the ultrasensitive detection of microRNA-141 (miRNA-141) combining target recycling amplification and the double-output conversion strategies. Notably, the proposed double-output conversion strategy enabled a small number of miRNA to be successfully transferred into a large number of reporter DNA which could capture numerous $QDs\text{-}Ru(dcbpy)_3^{2+}$-labeled signal probes on the sensing surface to realize the ECL response to the logarithm of the concentration of miRNA-141. With the ultrahigh-efficient ECL-RET in one nanostructure and the dual amplification including target recycling as well as double-output conversion strategies, the proposed biosensor realized ultrasensitive detection of miRNA-141 and performed the concentration range from 100 aM to 10 pM and the estimated detection limit was 33 aM (S/N=3). Impressively, this method

can sensitively detect the miRNA-141 of human prostate cancer cells and provide a significant boost for the detection of other biomarkers in early cancer diagnosis and therapeutic monitoring.

KEYWORDS: Electrochemiluminesce resonance energy transfer; Dual amplification; MicroRNA-141; Prostate cancer.

INTRODUCTION

Prostate cancer, which is often no early symptoms and extremely difficult to diagnose, has become the second most common cancer and ranked the fifth leading cause of cancer-related death in male[1, 2]. However, the mechanisms of the tumorigenesis and metastasis of prostate cancer that the cancer cells detach from the primary lesion to colonize distant sites are still largely unknown. Amazingly, it has been reported that certain microRNAs (miRNAs) connected to prostate cancer development, acting as cancer oncogenes or suppressors and employing as cancer biomarkers for early diagnosis of prostate cancer[3-5]. Additionally, previous studies have revealed that miRNA-141 overexpressed in prostate cancer cells[6] (22 Rv1 cell line). Therefore, sensitive detection of miRNA-141 from prostate cancer cells can provide significant information in terms of clinical analysis and therapy of prostate cancer. However, it is a realistic challenge to make ultrasensitive determination of miRNA owing to its inherent virtues of small size and low abundance in cancer cells[7]. Consequently, establishing a reliable and selective method for ultrasensitive miRNA analysis is essential to the development of early diagnosis in prostate cancer.

Electrochemiluminesce (ECL), known as a widely applicable analysis tool generated by electrochemical reactions between electrogenerated species, could be effectively applied in sensitive sand selective detection of miRNA result from its excellent controllability, low background and simplified optical setup[8-10]. In the multifarious fascinating ECL emitters, quantum dots (QDs) amazed the researchers on the horizon of widely used luminescent emitters for the reason of its stable physical and chemical properties, strong anti-interference capacity and easy film-forming[11-13]. However, the ECL efficiency is limited when QDs were directly applied in the detecting solution without any enhanced reagents. Besides, putting QDs in the detecting solution may waste the reagent and increase the cost, further restricting its ECL intensity due to the poor effective collision frequency. Therefore, the promotion of luminous efficiency of QDs is of great importance for the wide application of ECL biosensor. Conventionally, the ECL response greatly enhanced by the following two protocols. One is that the introduction of an applicable coreactant can enhance the ECL signal, which is extensively employed and already comparatively mature in the detection of miRNA[14, 15]. The other protocol is to adopt a suited energy donor to realize electrochemiluminesce resonance energy transfer (ECL-RET) for enhancing the ECL intensity of QDs, which has gained increasing interest in the trace analysis of miRNA biomarkers because ECL-RET has no excitation light source and no interference from the scattered light[16-18]. In the past decades, the researchers have focused on searching for desirable donor-acceptor pairs to improve the ECL efficiency of QDs. For instance, Zhang's group reported an ECL-RET system from luminol to

luminescent QDs on theAu working electrode for studying the interactions and conformational changes of proteins[19]. Recently, Zhu's group employed an efficient ECL-RET system between luminol donor and QDs acceptor for the construction of a thrombin protein biosensor[20]. Although these methods can enhance the luminous efficiency of QDs to some extent, the ECL response is still limited because the energy donor-acceptor pairs are different independent nanostructure, leading to more energy loss due to the long path of energy transmission. Therefore, we assume that controlling the donor-acceptor pairs within one nanostructure may greatly reduce the energy loss and improve the efficiency of energy transfer, further enhancing the ECL efficiency of QDs considerably.

The demand for miRNA determination is rapidly expanding for the low abundance of miRNA in cancer cells, which drives the researchers to explore attractive nucleic acid amplifications applied in sensitive bio-detection. Especially, the DNA nicking endonuclease, has emerged as a powerful role that applied in nucleic acid amplifications because it can cleave only one strand of DNA on a double stranded DNA (dsDNA) substrate[21-23]. For example, Zhang's group constructed a simple fluorescence biosensor by introducing DNA nicking endonuclease to achieve detection towards let-7a miRNA[24]. Recently, Jiang's group developed an isothermal nucleic acid amplification technology for miRNA determination by the employment of endonuclease IV to prime the DNA replication[25]. However, these approaches only acquired haploid reporter DNA on the account of that there was only one cleavage site on the complementary dsDNA, which limited the amplification efficiency and the

sensitivity of the elaborated biosensor. Hence, developing a novel efficient signal amplification strategy for assaying miRNA-141 is a hot issue in this research field.

Herein, a desirable high-efficient ECL-RET model with Tris (4,4'-dicarboxylicacid-2,2'-bipyridyl) ruthenium(II) dichloride ($Ru(dcbpy)_3^{2+}$) as the donor and CdSe@ZnS quantum dots (QDs) as the acceptor in one nanostructure was developed. By combining with an improved dual amplification including target recycling and double-output conversion strategies, an excellent ECL biosensor for the ultrasensitive detection of miRNA-141 was constructed based on the novel one nanostructure ECL-RET system. As shown in Scheme 1A, QDs were employed to load $Ru(dcbpy)_3^{2+}$ through amide bond with the realization of ECL-RET in one nanostructure (QDs-$Ru(dcbpy)_3^{2+}$). Furthermore, capture 1 was adopted as a probe anchor to form a novel ECL signal tag of QDs-$Ru(dcbpy)_3^{2+}$/capture 1 via amidation reaction. As displayed in Scheme 1B, the hairpin DNA 1 (H1) was opened by target miRNA-141, obtaining dsDNA with some exposed bases. Under the existence of hairpin DNA 2 (H2), the above dsDNA hybridized with H2 to replace the miRNA and realize the recycling of target miRNA, achieving a large number of dsDNA named template strand. With the aid of Bst 2.0 DNA polymerase (polymerase), H1 began to polymerize with the template of H2, generating a fully complementary dsDNA with two endonuclease-recognized sites. After the addition of nicking endonuclease Nt.BbvCI (Nt.BbvCI), the two specific cleavage sites were recognized and amounts of reporter DNA were achieved. Subsequently, the treated glassy carbon electrode (GCE) was dipped in $HAuCl_4$ solution, which gained an Au nanoparticles (AuNPs) film to assembled massive capture probe 2 (capture 2) through Au-S bond. Next, to block the nonspecific binding sites, hexanethiol (HT) was dropped onto the surface of proposed electrode. Furthermore, reporter DNA and QDs-$Ru(dcbpy)_3^{2+}$/capture 1 were

incubated onto the prepared GCE to capture the signal probes on the sensing surface by hybridizing with capture 2. In the end, the proposed ECL biosensor achieved the quantitative detection of miRNA-141 through the variation of ECL response proportion to the miRNA-141 concentration in a broad range from 100 aM to10 pM with the detecting limit of 33 aM. Significantly, the elaborated biosensor enabled to sensitively monitor miRNA-141 from human prostate cancer cells, which held key potential for the real application of early cancer diagnosis and clinical analysis.

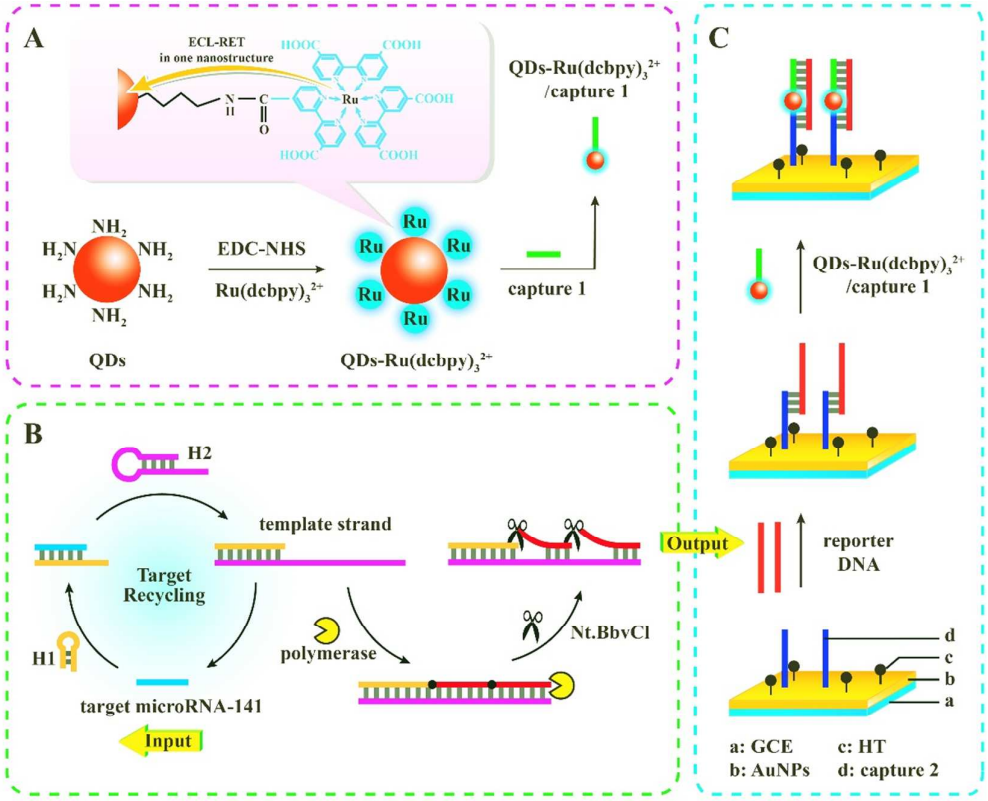

Scheme 1. The construction of the miRNA biosensor based on the novel high-efficient ECL-RET in one nanostructure. (A) The preparation of QDs-Ru(dcbpy)$_3^{2+}$/capture 1 bioconjugate and the mechanism of ECL-RET in one nanostructure; (B) The dual amplification assay including target recycling and double-output conversion strategies; (C) The establishment of the proposed biosensor.

EXPERIMENTAL SECTION

Dual amplification assay. 2 μM of H1 and 2 μM of H2 were heated separately to 95 °C for 3 min and cooled to 55 °C slowly in 60 min to form the hairpin structure, following by the addition of miRNA-141. Afterwards, the prepared solution was incubated for 3 h to obtain abundant production of the template strand. After that, 1.4 mM dNTPs and 32 U/mL polymerase were added to the mixture, which was performed at 65 °C for 60 min. Subsequently, 0.2 U/μL Nt.BbvCI was dropped immediately into the above reaction solution and it was heated at 45 °C for 60 min. In the end, the mixture was terminated by heating it at 80 °C for 20 min to realize the dual amplification strategy and obtain numerous reporter DNA.

Preparation of the composite of QDs-Ru(dcbpy)$_3^{2+}$/capture 1. Firstly, 100 μL mixture including 40 mM EDC and 10 mM NHS were added in Ru(dcbpy)$_3^{2+}$ (2 μM, 400 μL) and 400 μL of capture 1 (1 μM) respectively, then stirred at room temperature for 15 min. Next, QDs were added into the mixture of Ru(dcbpy)$_3^{2+}$and stirred for 1 h. Then, capture 1 solution was introduced into the proposed solution under stirring for 1 h to achieve QDs-Ru(dcbpy)$_3^{2+}$/capture 1. In the above process, EDC was used to active the carboxylic groups of capture 1 and Ru(dcbpy)$_3^{2+}$ and the function of NHS was employed to crosslink the activated carboxyl of capture 1/Ru(dcbpy)$_3^{2+}$ and the amino group of QDs. Then the mixture was centrifuged for several times and washed with double-distilled water twice to get rid of the supernatant. Finally, the above precipitate was dispersed in 400 μL of TAE/Mg^{2+} buffer as QDs-Ru(dcbpy)$_3^{2+}$/capture 1 for further use.

Construction of the proposed miRNA biosensor. A GCE was first polished with 0.3 μm and 0.05 μm α-Al_2O_3 slurry, respectively and ultrasonically cleaned in double-distilled water and ethanol. Afterwards, the bare GCE was dried in air and successively electrodeposited in 1% $HAuCl_4$ solution under the potential of -0.2 V for 30 s to achieve AuNPs platform. Next, 10μL of 1 μM capture 2 was fabricated on the above modified electrode through Au-S bond for 12 h. After being rinsed by double-distilled water and dried in the air, 1.0 mM of HT was added on the sensing surface for 40 min to block the remaining binding sites. Then, 10 μL mixture of reporter DNA and 10 μL of QDs-$Ru(dcbpy)_3^{2+}$/capture 1 were dropped on modified electrode surface for 2 h in the dark environment. Finally, the incubated GCE was chairily rinsed with double-distilled water and was detected in 0.05 M $S_2O_8^{2-}$.

RESULTS AND DISCUSSION

The demonstration of ECL-RET between $Ru(dcbpy)_3^{2+}$ and QDs. In order to prove the ECL-RET between $Ru(dcbpy)_3^{2+}$ as the donor and QDs as the acceptor, the UV-vis absorption spectra of QDs and the ECL emission spectra of $Ru(dcbpy)_3^{2+}$ were studied with the cyclic potential scanning from -1.6 to 0 V. As showed in Figure 1A, the maximum of ECL emission peak of $Ru(dcbpy)_3^{2+}$appeared at 617 nm (curve b) and the UV-vis absorption peak of QDs was observed in the scope of 570-660 nm (curve a). It can be seen that the UV-vis absorption spectra of QDs (curve a) overlapped well with the ECL emission spectra of the $Ru(dcbpy)_3^{2+}$ (curve b), which demonstrated the possibility of ECL-RET between $Ru(dcbpy)_3^{2+}$ and QDs.

To further clarification of the ECL-RET between the $Ru(dcbpy)_3^{2+}$ donor and the

QDs acceptor, ECL response of different modified electrodes were studied. An ECL peak of sole QDs can be observed and the consequence was shown in Figure 1B (curve a). However, a significant ECL response of the QDs-$Ru(dcbpy)_3^{2+}$ composite can be achieved (curve b), comparing with the ECL peak of sole QDs. With the obtained experimental data, it could be concluded that the ECL-RET would occur between $Ru(dcbpy)_3^{2+}$ and QDs, where $Ru(dcbpy)_3^{2+}$ emitted short wavelength as the energy donor and QDs emitted long wavelength as the acceptor.

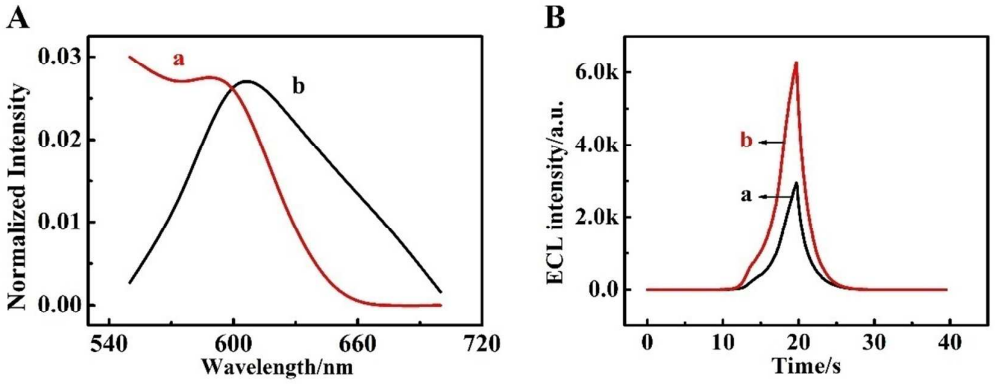

Figure 1. (A) UV-vis absorption spectra of QDs (curve a) and the ECL emission response of $Ru(dcbpy)_3^{2+}$ (curve b). (B) The ECL response of QDs (curve a) and the composite of QDs-$Ru(dcbpy)_3^{2+}$ (curve b).

The ECL spectra of $Ru(dcbpy)_3^{2+}$, QDs and the composite of QDs-$Ru(dcbpy)_3^{2+}$ have been made by gathering the maximum ECL response during the cyclic potential sweep with a series of optical filters. As illustrated in the following Figure 2, the ECL emission peak of QDs appeared at 641 nm (Figure 2A) and the ECL spectra peak corresponding to $Ru(dcbpy)_3^{2+}$ was located at 617 nm (Figure 2B). Meanwhile, as shown in Figure 2C, when the composite of QDs-$Ru(dcbpy)_3^{2+}$ was added in the detecting solution solely, there existed dual ECL spectra peak, one low peak value

corresponding to $Ru(dcbpy)_3^{2+}$ and the other high peak value corresponding to QDs. The obtained results demonstrated that the ECL-RET in one nanostructure between QDs and $Ru(dcbpy)_3^{2+}$, namely energy transfer from the higher-band gap $Ru(dcbpy)_3^{2+}$ to the lower-band gap QDs, was highly efficient.

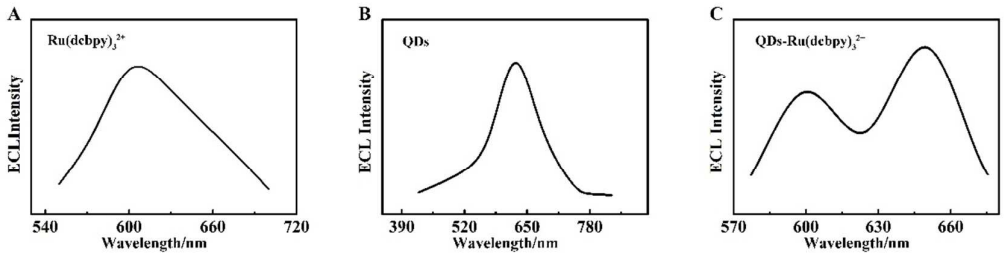

Figure 2. ECL spectra of (A) $Ru(dcbpy)_3^{2+}$; (B) QDs and (C) QDs-$Ru(dcbpy)_3^{2+}$ composite.

In order to demonstrate the high efficient of ECL-RET, ECL response of the composite of QDs-$Ru(dcbpy)_3^{2+}$, and the independent QDs and $Ru(dcbpy)_3^{2+}$ in the detecting solution were detected with same concentration. As presented in Figure 3, it could be found that the QDs-$Ru(dcbpy)_3^{2+}$ composite (curve a) showed a higher ECL response than the independent QDs with $Ru(dcbpy)_3^{2+}$ (curve b), which would be due to the shorter transition path and the higher ECL-RET efficiency. Furthermore, when QDs and $Ru(dcbpy)_3^{2+}$ were controlled in one nanostructure, the ECL peak appeared 0.1 s earlier than the independent QDs with $Ru(dcbpy)_3^{2+}$. These results manifested that QDs-$Ru(dcbpy)_3^{2+}$ composite could significantly reduce the energy loss and improved ECL efficiency of QDs because of the short path of energy transmission.

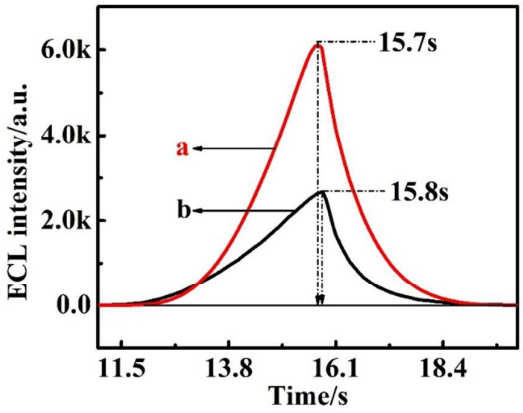

Figure 3. ECL dynamic curve of (a) QDs-Ru(dcbpy)$_3^{2+}$ composite; (b) Independent QDs with Ru(dcbpy)$_3^{2+}$.

Electrochemical characterization of the designed miRNA biosensor. To confirm the successful stepwise fabrication process of the miRNA biosensor, the cyclic voltammograms (CVs) were employed in 5.0 mM $[Fe(CN)_6]^{3-/4-}$ from -0.2 to 0.6 V at a scan rate of 0.1 V s^{-1}. As can be seen in Figure 4, the bare GCE exhibited a pair of quasi-reversible redox peaks of $[Fe(CN)_6]^{3-/4-}$ (curve a). After AuNPs were electrodeposited on the surface of bare GCE, an apparent increase in redox current was obtained because the well electrical conductivity of AuNPs could promote electron transfer (curve b). Whereas the capture 2 was immobilized onto the prepared electrode, an obviously decreased current was detected due to the characteristic of impeding the electron transfer of DNA (curve c). Subsequently, the redox peak integrally decreased when the successive immobilization of HT on the electrode (curve d). After adding the reporter DNA and QDs-Ru(dcbpy)$_3^{2+}$/capture 1 to the modified sensor, an further decrease of the redox current appeared (curve e) for that the DNA structure could inhibit the electron transfer. The results characterized the CVs performance of the proposed ECL biosensor construction.

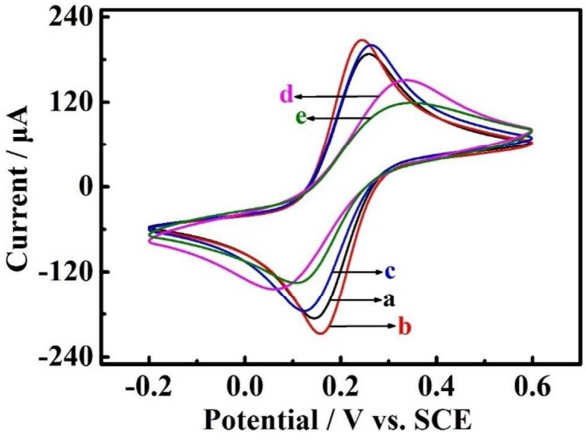

Figure 4. Typical CVs of the modified electrode performed in 5.0 mM $[Fe(CN)_6]^{3-/4-}$ with the scan range of -0.2 to 0.6 V. (a) Bare GCE; (b) GCE/AuNPs, (c) GCE/AuNPs/capture 2; (d) GCE/AuNPs/capture 2/HT; (e) GCE/AuNPs/capture 2/HT/QDs-Ru(dcbpy)$_3^{2+}$/capture 1 and reporter DNA.

The experimental optimization of the miRNA biosensor. The incubation time and temperature of Nt.BbvCI were critical to the performance of the referred biosensor. Therefore, the optimal incubation time of the Nt.BbvCI has been assessed to present an improved miRNA biosensor. The analytical data was shown in Figure 5A, under the different incubation time of Nt.BbvCI, the ECL signal was determined at the range from 30 to 90 min. The ECL signal gradually increased along with the growth of the incubation time and reached the maximum at 60 min. Therefore, the optimal incubation time was 60 min in this work.

Furthermore, to investigate the satisfying incubation temperature of Nt.BbvCI, the ECL intensity of the sensing platform was detected with the different incubation temperature of Nt.BbvCI in the presence of 0.05 M $S_2O_8^{2-}$. As depicted in Figure 5B, with the increasing of incubation temperature from 25 ℃ to 60 ℃, the ECL signal

increased and went fora maximum value at 45 ℃, and then the signal decreased along with the increase of incubation temperature. Hence, 45 ℃ was selected as the fixed incubation temperature in the experiment.

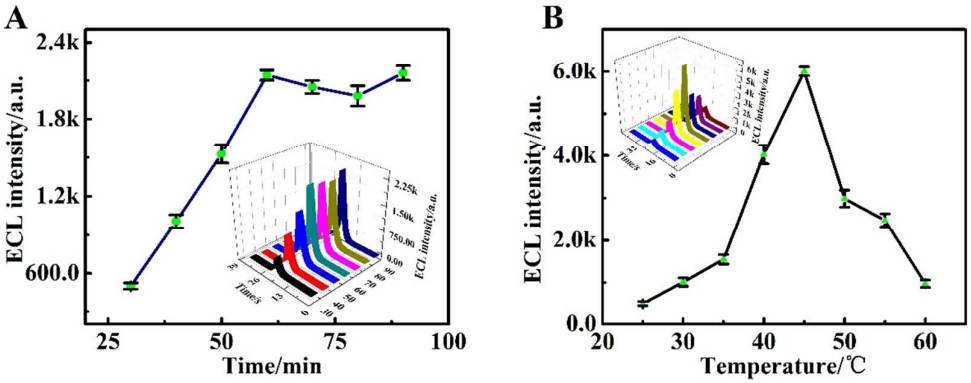

Figure 5. (A) Effect of the Nt.BbvCI incubation time on the ECL response of the miRNA biosensor recorded in 0.05 M $S_2O_8^{2-}$. (B) Effect of the Nt.BbvCI incubation temperature on the ECL response of the proposed biosensor in 0.05 M $S_2O_8^{2-}$.

Considerably, the factor of the concentration of the QDs-Ru(dcbpy)$_3^{2+}$/capture 1 and the capture 2 also directly affected the performance of the miRNA biosensor. To achieve the optimal concentration of the QDs-Ru(dcbpy)$_3^{2+}$/capture 1 and the capture 2, we have investigated the optimal concentration of the above nanomaterials and the ratio of the concentration of QDs-Ru(dcbpy)$_3^{2+}$/capture 1 and capture 2 was controlled with 1:1 in advance. From Figure 6, it could be observed that the ECL response increased apparently as the increasing concentration of QDs-Ru(dcbpy)$_3^{2+}$/capture 1 and capture 2 from 0.1 μM to 4 μM. When the concentration of the mixture was greater than 1 μM, the ECL response reached a relative stabilized value and 1 μM was chosen as the ideal concentration of the reaction system.

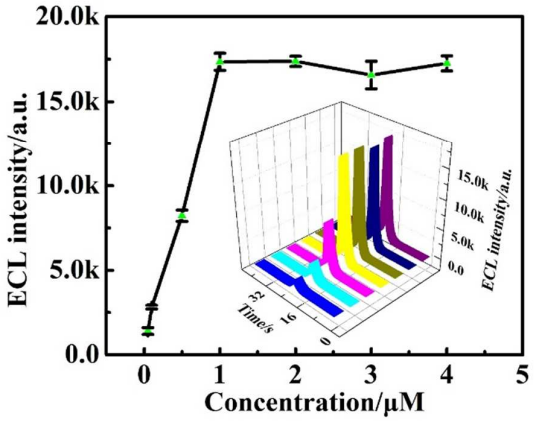

Figure 6. Effect of the concentration of QDs-Ru(dcbpy)$_3^{2+}$/capture 1 and capture 2 on the ECL response of the miRNA biosensor recorded in 0.05 M $S_2O_8^{2-}$.

Analytical performance of the miRNA biosensor. Under the optimal condition, the ECL response gradually increased with the increasing concentration of the miRNA-141 (Figure 7A). As displayed in Figure 7B, in the linear range from 100 aM to 10 pM, the linear regression equation was I = 13786.27 + 3354.67 lg c, with a correlation coefficient R of 0.9976. The detection limit was 33 aM (S/N = 3), suggesting a remarkable linear relationship between logarithm of the miRNA-141 concentration and ECL signal. Significantly, the working performance of the designed miRNA biosensor for miRNA-141 analysis is comparable and even better than the previous ones and the corresponding data was shown in table 1.

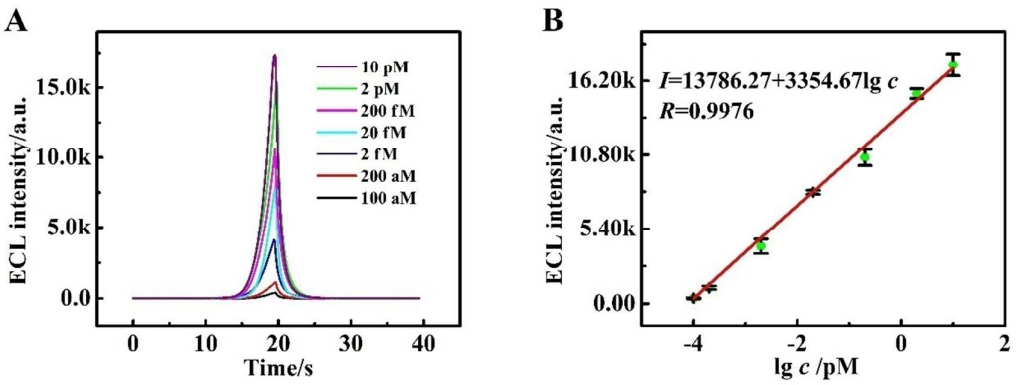

Figure 7. (A) Typical ECL response of the referred miRNA biosensor introduced with different concentrations of miRNA-141 recorded in 0.05 M $S_2O_8^{2-}$. (B) Calibration curve for the various logarithm concentrations of miRNA-141.

Table 1. The comparison of the present biosensor with the previous analytical strategies.

Method	Target	Detection limit	Dynamic range	References
Electrochemical	miRNA	10 fM	5 fM to 5 pM	26
Fluorescent	miRNA	1.5 fM	1.5 fM to 9 fM	27
Fluorescent	miRNA	1 fM	1 fM to 100 nM	28
ECL	miRNA	10 fM	10 fM to10 pM	29
ECL	miRNA	500 aM	1 fM to 1 nM	30
ECL	miRNA	33 aM	100 aM to 10 pM	This study

The specificity, stability and reproducibility of the elaborated miRNA biosensor. The detection of unique miRNA was a great challenge, because they currently coexisted with other miRNAs including miRNA-21 and miRNA-155, which had high similarity of length and sequence[31-33]. To explore the selectivity of the

elaborated miRNA biosensor by comparing the ECL response of the obtained method toward the target miRNA-141 against miRNA-21 and miRNA-155 sequence, the interfering substances including miRNA-21 (10 pM) and miRNA-155 (10 pM) were used to replace 0.1 pM of miRNA-141, respectively. As depicted in Figure 8A, after incubating target miRNA-141 (0.1 pM) onto the biosensor, the ECL signal increased sharply compared with the blank sample. While when the biosensor was added with miRNA-21 or miRNA-155, the ECL signal was insignificant and similar to the blank sample. As expected, compared to the target miRNA-141, the mixture of the target miRNA-141 (0.1 pM) with the above interfering agents (each at 10 pM) had the same effect with the target miRNA-141 on the ECL response. The experimental results showed that the influence of miRNA-21 and miRNA-155 on ECL signal could be ignored, and the biosensor for miRNA-141 detection exhibited remarkable specificity.

The stability of the obtained biosensor was applied in the detection of 2 pM of miRNA-141 under the optimal conditions. As shown in Figure 8B, the prepared biosensor was continuously scanned for 20 cycles and yielded a good stability with the relative standard deviation (RSD) of 1.05%, which suggested the significant accuracy of the biosensor. The reproducibility of mentioned biosensor is another imperative performance for the detection of miRNA-141. Therefore, the reproducibility of this ECL biosensor was studied using three different modified electrodes for determination and the RSD was 4.02%. Furthermore, the same biosensor was repeatedly analyzed in consecutive three days and the inter-assay of RSD as 4.56%. As a result, the biosensor possessed an excellent stability and

reproducibility.

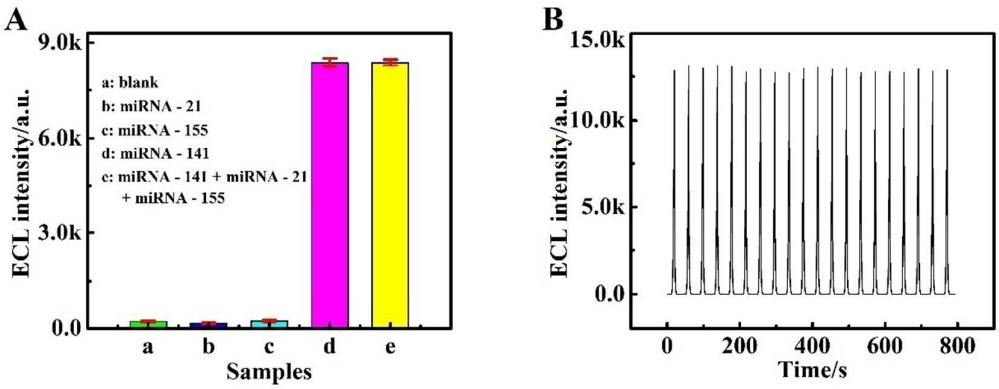

Figure 8. (A) The specificity of the mentioned miRNA biosensor: (a) blank, (b) miRNA-21 (10 pM), (c) miRNA-155 (10 pM), (d) miRNA-141 (0.1 pM), (e) the mixture of miRNA-141 (0.1 pM), miRNA-21 (10 pM) and miRNA-155 (10 pM). (B) The stability of themiRNA biosensor with ECL intensity-time curve in the optimal conditions under consecutive cyclic potential scans for 20 cycles.

Analysis of the miRNA-141 in cancer cells. The clinical application of the proposed miRNA biosensor for practical samples was investigated by detecting the total miRNA from two different human cancer cells including 22 Rv1 (human prostate cancer cells) and HeLa (human cervical cancer cells) cancer cells. As depicted in Figure 9, the ECL signal increased with the increasing of 22 Rv1 cell numbers, while the ECL signal exhibited a relatively low response with the increasing of HeLa cell numbers. The above results indicated that miRNA-141 had a high expression in 22 Rv1 cancer cells and a low expression in HeLa cancer cells, which were consistent to the previous reports[34]. It can be concluded that the presented ECL biosensor showed a key potential in the application of clinical analysis in early cancer diagnostics and biomedical research.

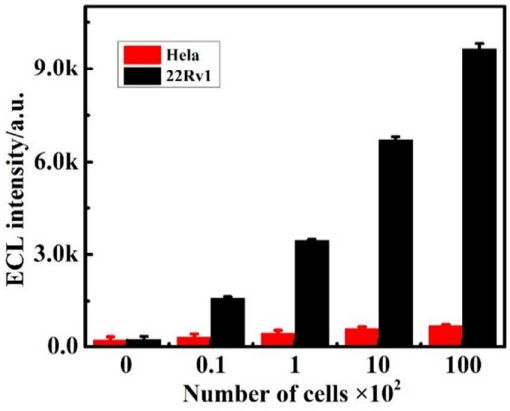

Figure 9. ECL response corresponding to the miRNA-141 in diverse cell numbers of Hela (red bars) and 22 Rvl (black bars) human cancer cells.

CONCLUSIONS

In summary, a high-efficient ECL-RET system within one nanostructure was studied and applied to construct a reliable biosensor for the ultrasensitive detection of miRNA-141. This work brings forth two original ideas as following. Firstly, a novel ECL-RET model within one nanostructure containing the donor of $Ru(dcbpy)_3^{2+}$ and the acceptor of QDs was developed for the first time, which significantly reduced the energy loss and improved the ECL efficiency of QDs because of the short path of energy transmission. Secondly, the introduction of the improved dual amplification including target recycling and double-output conversion strategies realized a small number of miRNA to be transferred into a large number of reporter DNA, which amplified the signal of the target and caused the remarkably enhancement of the related ECL intensity. With the combination of the novel high-efficient ECL-RET in one nanostructure and the excellent dual amplification, the proposed biosensor realized the ultrasensitive detection of miRNA-141 down to 33 aM and could be used

for monitoring the miRNA-141 from human prostate cancer cells sensitively. Moreover, the proposed biosensor could be applied as a universal tool for realizing the detection of other cancers biomarkers by changing the corresponding sequences of the hairpin DNA H1 and H2, which provided a new pathway for the application of early cancer diagnosis and clinical analysis.

ASSOCIATED CONTENT

Supporting Information

Optical spectrum characterization of the ECL-RET between $Ru(dcbpy)_3^{2+}$ and QDs, comparision of different amplification strategies based miRNA biosensor, reagents and materials, and apparatus are provided as Supporting Information. This information is available free of charge via the Internet at http://pubs.acs.org.

AUTHOR INFORMATION

Corresponding Authors

*Tel.: +86-23-68252277; Fax: +86-23-68253172.

E-mail address: yqchai@swu.edu.cn (Y. Q. Chai), yuanruo@swu.edu.cn (R. Yuan)

Notes

The authors declare no competing financial interest.

ACKNOWLEDGMENT

This work was financially supported by the National Natural Science Foundation (NNSF) of China (Grants 21675129, 21575116 and 51473136) and the Fundamental Research Funds for the Central Universities (Grant XDJK2016E055), China.

REFERENCES

(1) Permuthwey, J.; Thompson, R. C.; L Nabors, Burton.; Olson, J. J.; Browning, J. E.; Madden, M. H.; Chen, Y. A.; Egan, K. M. *The Pro*state **2010**, *70*, 467-472.

(2) Servian, P.; Celma, A.; Planas, J.; Placer, J.; Torres, I. D.; Olivan, M.; Morote, J. *The Prostate* **2016**, *76*, 1501-1506.

(3) Plasterk R. H. *Cell* **2006**, *124*, 877-881.

(4) Bentwich I.; Avniel A. Karov Y.; Aharonov R.; Gilad S.; Barad O.; Barzilai A.; Einat P.; Einav U.; Meiri E.; Sharon E.; Spector Y.; Bentwich Z.; *Nat. Genet*. **2005**, *37*, 766-770.

(5) Calin G. A.; Croce C. M.; *Nat. Rev. Cancer* **2006**, *6*, 857-866.

(6) Li, X.; Li, D. X.; Zhou, W. J.; Chai, Y. Q.; Yuan, R.; Xiang, Y. *Chem. Commun.* **2015**, *51*, 11084-11087.

(7) Baker M.; *Nat. Methods* **2010**, *7*, 687-692.

(8) Irkham, Watanabe T.; Fiorani A.; Valenti G.; Paolucci F.; Einaga Y. *J. Am. Chem. Soc.* **2016**, *138*, 15636-15641.

(9) Richter M. M. *Chem. Rev.* **2004**, *104*, 3003-3036.

(10) Liu Z. Y.; Qi W. J.; Xu G. B. *Chem. Soc. Rev*. **2015**, *44*, 3117-3142.

(11) Dong Y. Q.; Pang H. C.; Yang H. B.; Guo C. X.; Shao J. W.; Chi Y. W.; Li C. M.; Yu T. *Angew. Chem. Int. Ed*. **2013**, *52*, 7800-7804.

(12) Medintz I. L.; Clapp A. R.; Mattoussi H.; Goldman E. R.; Fisher B.; Mauro J. M. *Nat*. *Mater*. **2003**, *2*, 630-638.

(13) Martín-Yerga, D.; Rama E. C.; Costa-García A. *Anal*. *Chem*. **2016**, *88*, 3739-3746.

(14) Deiss F.; LaFratta C. N.; Symer M.; Blicharz T. M.; Sojic N.; Walt D. R. *J. Am. Chem. Soc.* **2009**, *131*, 6088-6089.

(15) Zheng L. Y.; Chi Y. W.; Dong Y. Q.; Lin J. P.; Wang B. B. *J. Am. Chem. Soc.* **2009**, *131*, 4564-4565.

(16) Zhao H. F.; Liang R. P.; Wang J. W.; Qiu J. D. *Chem. Commun.* **2015**, *51*, 12669-12672.

(17) Gao Z. Q.; Deng H. M.; Shen W.; Ren Y. Q. *Anal. Chem.* **2013**, *85*, 1624-1630.

(18) Zhang H.; Wang Y. S.; Zhao D. W.; Zeng D. D.; Xia J. Y.; Aldalbahi A. L.; Wang C. G.; San L. L.; Fan C. H.; Zuo X. L.; Mi X. Q. *ACS Appl. Mater. Interfaces* **2015**, *7*, 16152-16156.

(19) Li L.; Li M. Y.; Sun Y. M.; Li J.; Sun L.; Zhou G. Z.; Zhang X. L.; Jin W. R.; *Chem. Commun*. **2011**, *47*, 8292-8294.

(20) Dong Y. P.; Gao T. T.; Zhou Y.; Zhu J. J.; *Anal. Chem*. **2014**, *86*, 11373-11379.

(21) Sun X. Y.; Wang L.; Zhao M. S.; Zhao C. Z.; Liu S. F.; *Chem. Commun*. **2016**, *52*, 11108-11111.

(22) Ali M. M.; Aguirre S. D.; Lazim H.; Li Y. F. *Angew. Chem. Int. Ed*. **2011**, *50*, 3751-3754.

(23) Yang L. L.; Tao Y. Z. Yue G. Y.; Li R. B.; Qiu B.; Guo L. H.; Lin Z. Y.; Yang H. H. *Anal. Chem*. **2016**, *88*, 5097-5103.

(24) Wang G. L.; Zhang C. Y.; *Anal. Chem*. **2012**, *84*, 7037-7042.

(25) Zhou D. M.; Du W. F.; Xi Q.; Ge J.; Jiang J. H. *Anal. Chem*. **2014**, *86*, 6763-6367.

(26) Koo K. M.; Carrascosa L. G.; Shiddiky M. J. A.; Trau M. *Anal. Chem.* **2016**, *88*, 2000-2005.

(27) Tang Y. Q.; He X.; Zhou Z. X.; Tang J. K.; Guo R.; Feng X. L. *Chem. Commun*. **2016**, *52*, 13905-13908.

(28) Duan X.; Zuo X. L.; Wang S. T.; Quan X. Y.; Chen D. L.; Chen Z. F.; Jiang L.; Fan C. H.; Xia F. *J. Am. Chem. Soc.* **2013**, *135*, 4604-4607.

(29) Liao, Y. H.; Huang, R.; Ma, Z. K.; Wu, Y. X.; Zhou, X. M.; Xing, D. *Anal. Chem.* **2014**, *86*, 4596−4604.

(30) Feng Q. M.; Shen Y. Z.; Li M. X.; Zhang Z. L.; Zhao W.; Xu J. J.; Chen H. Y. *Anal. Chem.* **2016**, *88*, 937-944.

(31) Moltzahn F.; Olshen A. B.; Baehner L.; Peek A.; Fong L.; Stoppler H.; Simko J.; Hilton J. F.; Carroll P.; Blelloch R. *Cancer Res.* **2011**, *71*, 550-560.

(32) Patolsky F.; Zayats M.; Katz E.; Willner I. Zhu J.; Wang S. G.; Zhang W. Y.; Qiu J. Y.; Shan Y. X.; Yang D. R.; Shen B. R. *Oncotarget* **2015**, *6*, 43819-43830.

(33) Cai Z. K.; Chen Q.; Chen Y. B.; Gu M.; Zheng D. C.; Zhou J. Wang Z. Molecular Medicine Reports **2015**, *11*, 533-538.

(34) Mitchell P. S.; Parkin R. K.; Kroh E. M.; Fritz B. R.; Wyman S. K.; PogosovaAgadjanyan E. L.; Peterson A.; Noteboom J.; O'Briant K. C.; Allen A.; Lin D. W.; Urban N.; Drescher C. W.; Knudsen B. S.; Stirewalt D. L.; Gentleman R.; Vessella R. L.; Nelson P. S.; Martin D. B.; Tewari M. *Proc. Natl. Acad. Sci. U. S. A.* **2008**, *105*, 10513-10518.

for TOC only

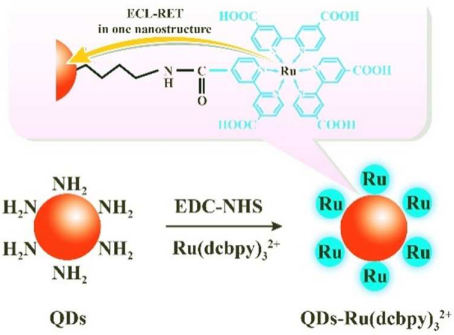
ECL-RET
in one nanostructure
HOOC
COOH
Ru
COOH
HOOC
COOH
N
H
C
O
NH2
H2N
NH2
H2N
NH2
EDC-NHS
Ru(dcbpy)3 2+
Ru
Ru
Ru
Ru
Ru
QDs
QDs-Ru(dcbpy)3 2+